

This study investigates hydrostatic-dynamic processes in the hydrostatic-dynamic bearing of satellites in the aviation gearbox of a turboprop engine. The task addressed is to determine the influence of design parameters of a multi-chamber hydrostatic bearing on its basic characteristics taking into account the pressure of the working fluid and the diameter of the nozzle at the inlet to the bearing chambers. The basic characteristics considered are the bearing capacity, the flow rate of the working fluid, and the power loss due to friction. The basis for defining these characteristics is the pressure distribution function in the working fluid layer.

The influence of the working fluid pressure and the diameter of the nozzle at the inlet to the bearing chambers on the basic characteristics of the hydrostatic-dynamic bearing of the satellite of the aviation gearbox has been studied.

It has been established that the required bearing capacity for the selected design and adopted dimensions of the hydrostatic-dynamic bearing is provided at a pressure at the inlet to the bearing chambers of approximately 3 MPa. The value of the bearing capacity at a pressure of 3 MPa is 5438 N. The flow rate of the working fluid at this pressure does not exceed 0.0011 m³/s, or 1.1 l/s. The total power losses due to friction and pumping are approximately 6 kW. With an engine power of 1876 kW, the power losses on 4 satellite bearings are approximately 1.28% of the total engine power.

The results are obtained with a nozzle diameter at the inlet to the bearing chambers of 2.5 mm. Such a nozzle diameter allows for reliable operation of the hydrostatic-dynamic bearing under various operating modes.

The findings show that by selecting the design and operational parameters, the hydrostatic-dynamic bearing provides the necessary bearing capacity of the supports of satellites in aircraft gearboxes. Power losses from the use of hydrostatic bearings in the satellites of the aircraft gearbox practically do not affect the total power of the turboprop engine

Keywords: support, satellites, aviation gearbox, bearing chamber, jet, pressure, working fluid

UDC 621.822.5.032:532.517.4

DOI: 10.15587/1729-4061.2026.364308

REVEALING THE INFLUENCE OF DESIGN AND OPERATIONAL PARAMETERS ON THE CHARACTERISTICS OF A HYDROSTATIC BEARING IN AVIATION GEARBOX SATELLITES

Vladimir Nazin

Doctor of Technical Sciences, Professor

Department of Theoretical Mechanics,

Machine Science and Robotics

National Aerospace University

"Kharkiv Aviation Institute"

Vadima Manka str., 17, Kharkiv, Ukraine, 61070

E-mail: nazin.vlad11@gmail.com

ORCID: <https://orcid.org/0000-0002-7872-5429>

Received 18.03.2026

Received in revised form 29.05.2026

Accepted 09.06.2026

Published 29.06.2026

How to Cite: Nazin, V. (2026). Revealing the influence of design and operational parameters on the characteristics of a hydrostatic bearing in aviation gearbox satellites. *Eastern-European Journal of Enterprise Technologies*, 3 (7 (141)), 50–57. <https://doi.org/10.15587/1729-4061.2026.364308>

1. Introduction

The performance of the turboprop engine gearbox depends on the reliable operation of the supports for satellite gears. Initially, two rows of rollers were used in the satellite supports on each satellite. But the current trend towards increasing the rotor speeds of modern machines requires the consideration of higher-speed supports for the satellite gears of aircraft gearboxes. One of the options for solving this task is the use of fluid friction bearings, namely hydrostatic bearings, in the supports of the satellites in aircraft gearboxes.

Hydrostatic bearings occupy an important place in the classification of fluid friction bearings. One of the important advantages of hydrostatic bearings is the possibility of using the working body of the machine for the operation of the bearings. The turboprop engine is equipped with oil and fuel systems in which the working body is under pressure. The presence of working bodies under pressure is an additional factor that allows them to be used as working bodies in hydrostatic bearings. The operation of satellite bearings in the fluid friction mode makes it possible to virtually eliminate wear of the working surfaces of the bearing elements. This al-

lows for a significant increase in the reliability and resource of both the gearbox and the engine as a whole.

New operating conditions for rotor bearings of modern high-speed machines require designing new structures of sliding bearings, or the improvement of existing designs of sliding bearings of fluid friction.

Such bearings are hydrostatic-dynamic; they expand the range of stable operation on these bearings. Therefore, they are promising for high-speed machines.

Scientific research into this area is important because it makes it possible to assign the value of the working fluid pressure at the inlet to the hydrostatic-dynamic bearing and select the required diameter of the jets at the inlet to the bearing chamber in accordance with the required bearing capacity of the bearing. The use of hydrostatic bearings in the bearings of aircraft gearboxes is new and requires extensive theoretical and experimental research.

2. Literature review and problem statement

Work [1] considers increasing the specific power and reliability of wind turbine reducers in their low-speed stages

due to the use of sliding bearings. A thermal-elastic-hydrodynamic model for planetary plain bearings is proposed. Deformations are predicted using a self-programming procedure based on the finite element method. The mathematical model was tested experimentally. It was established that the corresponding deformation caused by the engagement could improve the performance of the sliding bearing, in case of misalignment due to the expansion of the bearing area. However, the work did not pay enough attention to the influence of the change in the dimensions of the bearing due to the increase in temperature.

Paper [2] examines the influence of the clearance in the bearing, external torque, and input speed on the vibrations of the planetary gear. Special attention was paid to the vibrations of a two-row planetary gear with a gap in the bearing. To solve this problem, a model of planetary gear transmission with six planetary bearings and one support bearing of the sun gear was built. In this methodology, a linear model of stiffness and damping of the system was considered. The influence of the clearance in the bearings and the external moment on the vibrations of the system was analyzed. The results of the study showed that by selecting the clearance in the bearing, it is possible to reduce system vibrations. However, the work does not pay attention to the construction of a nonlinear system vibration research model, which significantly affects the research results.

Planetary bearings of a two-planetary gear transmission are considered in work [3], due to their high bearing capacity. As supporting elements of planetary gears, they significantly influence the dynamics of the two-planetary gear transmission. The paper proposes an original time-varying wear model in a planetary bearing. The dynamic model includes bearing and gear excitation. The model is built using Archard's wear theory. The authors analyzed wear depth for different working times. The results of the experiments confirm findings on the basis of the constructed mathematical model. However, the work does not pay attention to the use of other types of bearings, which significantly reduce the wear of the working surfaces of the bearings.

In [4], the dynamic characteristics of a planetary gearbox due to localized defects in a sliding bearing are considered. A finite element dynamic model of a planetary gearbox is built. The defect profile is defined as rectangular. Gravity is also taken into account in the finite element model. The Coulomb friction model is used to describe the friction forces in a planetary gearbox. The simulation results were compared with the results using the previous method and could be used to simulate the dynamic characteristics of a sliding bearing. However, the work does not pay attention to the use of fluid friction in sliding bearings, which reduce the amount of wear.

In [5], an increase in torque density is considered by replacing a rolling bearing with a sliding bearing in wind turbine transmissions. Taking into account the elastic-hydrodynamic characteristics of sliding bearings of planetary gears, a rigid-flexible tribohydrodynamic model of a wind turbine transmission is built. The multi-objective optimization model of the gear wheel and bearing was solved using the developed algorithm. The effectiveness of the method was confirmed by the results of experiments. After optimizing the load displacement between the gear pairs, the edge contact in the bearings decreased, which significantly improved the vibration characteristics of the wind turbine gearbox. However, the work did not pay attention to taking into account the influence of the unbalance of the elements

of the analyzed system on the vibration characteristics of the wind turbine gearbox.

In work [6], to obtain high wind turbine power in gearboxes of large wind turbines, as an alternative to traditional rolling bearings, plain bearings are used in planetary gears. They are more reliable and have smaller dimensions. An experimental setup was designed to simulate the actual behavior of the lubricant. To obtain data on the film thickness, lubricant temperature, lubricant pressure, and friction torque, four piezoelectric elements, eight thermistors, two pressure sensors, and one torque sensor were used. To analyze the characteristics of the lubricant, under the established mode, under nominal conditions, three-dimensional values of pressure, temperature, and thickness of the lubricant were considered. The resulting experimental data were confirmed by numerical calculations. However, the work did not pay attention to the use of hydrostatic effects in the lubricant layer, in addition to hydrodynamic effects, which significantly reduce the total friction losses.

In [7], a combined model was built to study the dominant relationship between planetary bearings and planetary gearing. First, the planetary bearing is modeled, and then a refined combined dynamic model of the planetary gearing is built, which includes planetary gears, ring gear, carrier, sun gear, and planetary bearings. To verify the effectiveness of the model, a signal from a 2.0 MW air turbine installed at the operation site was used. The proposed model is recommended for fault analysis and fault diagnosis of the outer ring of a rolling bearing. However, the paper does not consider the use of fluid friction sliding bearings, which have a greater damping capacity than rolling bearings, to build a dynamic model.

In [8], the load on the satellite bearing of a planetary cycloidal reducer is considered, which determines the performance of the bearing. The paper reports an analysis of the change in the main load parameters on the gearbox. The gearbox was considered with a fixed input shaft and a rotating satellite. A computer experiment of the constructed mathematical model was carried out using the Mathcad package (USA). The analysis results revealed how the forces acting on the bearing change with increasing clearances at a constant torque on the output shaft. It was found that the operation of the gearbox is accompanied by a continuous change in the forces acting on the bearing. However, the work does not consider dynamic phenomena that necessarily arise with variable loads on the satellite bearings.

In [9], the increased requirements for the design of planetary gear bearings are considered, due to the increase in size and increased specific power. The use of plain bearings instead of rolling bearings in planetary gears has allowed the authors to increase the specific power and reliability of wind turbine bearings. The paper describes a highly effective calculation procedure, which is confirmed by pressure measurement data of a three-stage planetary gearbox of a powerful wind power plant. Analysis of the results reveals the need for further research in this area. However, the paper does not pay attention to the use of different types of plain bearings, such as fluid friction plain bearings, which reduce power losses due to friction. This is very important for powerful wind power plants.

In [10], the load distribution between several gears in planetary gears is considered. The study investigates the effect of the clearance in the bearings on the load distribution in the bearings using the analysis of the dynamics of multi-link systems. Nonlinear stiffness was used to express

the bearing clearance. The numerical method was verified by experiments in which the loads on the gear bearings were measured using strain gauges. The effect of the bearing clearance was also studied numerically. The results showed that the clearance in the guide is dominant. For a well-balanced load distribution, an appropriate clearance is proposed. However, the paper does not pay attention to the dynamic phenomena in the bearings but only considers the dynamics of gear engagement.

In [11], the deformation of the planetary gear and its bearing is considered. In this paper, the effect of the rim thickness on the load and the service life of the bearing is investigated. The analysis was carried out using a finite element model of the planetary gear rim with an integrated cylindrical roller bearing. Based on the obtained deformation of the planetary gear, the load distribution on the rolling elements in the bearing and the service life of the bearing were estimated. However, the work does not pay attention to the use of fluid friction sliding bearings, which significantly increase the service life of the bearings and the planetary gearbox in general.

In [12], the load distribution and fatigue life of various wind turbine gearboxes under rotor torque are investigated. Two planetary gear bearing configurations were compared: one used cylindrical roller bearings and the other preloaded tapered roller bearings. The study showed that the fatigue life of eight combined bearings of a planetary gearbox with preloaded tapered roller bearings is 3.5 times longer than that of a gearbox with cylindrical roller bearings. However, the study did not pay attention to the comparison with a planetary gearbox in which fluid friction bearings are used. They significantly increase the fatigue life of the planetary gearbox.

In [13], a computational model was built to assess the effect of wear on the characteristics of an engine bearing. The model takes into account the change in film thickness under dynamic loading due to wear of the bearing surface and shaft displacement. A method for estimating engine bearing wear is proposed, which ensures long-term operation and prevents its failure. The simulation shows that the contact pressure is significantly less than the hydrodynamic pressure, and a small decrease in the surface roughness of the bearing significantly reduces wear. However, the work does not pay attention to the use of hydrostatic bearings, which ensure wear-free operation of the bearing.

In [14], the influence of the deformation of the thin-walled structure of the planetary gear on the load distribution on the bearing is considered. Using the three-dimensional theory of curved beams by Tymoshenko and the transfer matrix method, a new analytical model was built that calculates the deformation of the planetary gear rim and the load on the bearing. The model was verified using finite element modeling. The results of the study showed that the deformation of the planetary gear rim significantly affects the contact load, pressure distribution and bearing service life. However, the paper does not pay attention to the effect of planetary gear rim deformation on bearing characteristics.

In summary, no attention in the reviewed literature [1–14] was paid to the possibility of using hydrostatic bearings in the supports of satellite gears in aircraft gearboxes. The use of these supports makes it possible to improve their load-bearing capacity and speed, as well as to increase the service life of the turboprop engine.

The above allows me to state that it is advisable to conduct a study on the influence of design and operational parameters on the characteristics of the hydrostatic bearing.

3. The aim and objectives of the study

The purpose of this work is to identify the influence of design and operational parameters on the characteristics of the hydrostatic-dynamic bearing of the satellite in the aircraft engine gearbox. This could make it possible to establish values for the design and operational parameters of the hydrostatic-dynamic bearing, which would ensure its required load-bearing capacity.

To achieve the goal, the following tasks were set:

- to determine the basic characteristics of hydrostatic-dynamic bearings taking into account hydrodynamic and hydrostatic effects;
- to study the influence of the nozzle diameter on the basic characteristics of the hydrostatic-dynamic bearing of the satellite in a gearbox.

4. The study materials and methods

The object of this study is the hydrostatic processes in a hydrostatic bearing of the satellites in the aviation gearbox of a turboprop engine. The principal hypothesis assumes the possibility of using hydrostatic bearings in the supports of satellites in turboprop engines.

Adopted assumptions:

- the flow of the lubricant is isothermal;
- the lubricant is an incompressible Newtonian fluid;
- there is no cavitation in the working fluid;
- the pressure gradients along the film thickness are small compared to the pressure gradients in other directions;
- the pressure in the chambers is the same on all surfaces;
- the thickness of the lubricant layer is small compared to the radii and length of the bearing; therefore, the curvature of the bearing surfaces can be neglected, and Cartesian coordinates can be used instead of curvilinear ones;
- the inertial terms of the Navier-Stokes equations are small compared to the viscous ones.

When constructing a mathematical model, assumptions generally accepted in the hydrodynamic theory of lubrication were adopted.

The calculations were performed for the case of a constantly acting external force, that is, in a stationary statement. The calculations were carried out in the Excel program (developed by Microsoft USA).

The structure of a satellite support with a hydrostatic bearing was designed (Fig. 1).

In the given structural diagram of the satellite support, the hydrostatic support has two rows of supporting chambers 1, into which the working fluid is supplied under high pressure P_1 . Each row has four supporting chambers. At the entrance to the chambers, inlet pressure compensators (jets) 2 are installed. After passing through the slotted path of the bearing, the liquid enters the drain through channels 3.

The lubricant is supplied through channels made in the axis of satellite 4. Satellite 5 has gear ring 6. On the right, plugs 7 are installed in the working fluid supply channel. The basis for determining the bearing capacity of the hydrostatic bearing, fluid consumption, and power losses due to friction and pumping was the pressure distribution function in the lubricant layer. The pressure in the lubricant layer was determined from the joint solution to the Reynolds equations and the balance of the working fluid consumption.

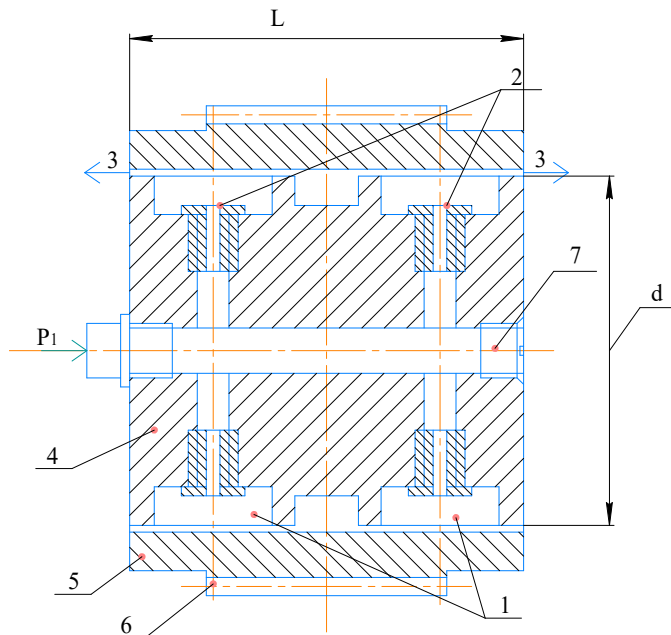


Fig. 1. Structural diagram of a satellite support with a hydrostatic bearing: 1 – bearing chambers; 2 – jets; 3 – drain channels; 4 – satellite axis; 5 – satellite; 6 – gear ring; 7 – plugs; d – bearing diameter; L – bearing length; P₁ – working fluid pressure

The pressure in the chambers was determined from the balance of the working fluid consumption, which was recorded from the condition of equality of the fluid consumption through the input compensating devices and the fluid consumption along the contour of the *i*-th chamber [15, 16].

The fluid consumption along the contour of the *i*-th chamber was recorded taking into account the transferred and gradient flow of the lubricant. The system of equations for determining the pressure in the chambers in a dimensionless form adapted for numerical implementation takes the following form

$$\begin{aligned} \left(\overline{P}_{k,i}\right)_{n+1} &= \overline{a}_{9,i} \cdot \sqrt{1 - \left(\overline{P}_{k,i}\right)_n} + \overline{a}_{11,i} \cdot \left(\overline{P}_{k,i-1}\right)_n + \\ &+ \overline{a}_{10,i} \cdot \left(\overline{P}_{k,i+1}\right)_n + \overline{a}_{10,i}, \end{aligned} \quad (1)$$

where $\overline{a}_{9,i}, \overline{a}_{11,i}, \overline{a}_{12,i}, \overline{a}_{10,i}$ are auxiliary coefficients that do not change during the iteration process.

Given the initial values of pressures in the chambers, new values of the pressures are obtained at step *n* + 1 according to equation (1). The iterative process continues until the required accuracy of determining the pressures in the chambers is achieved.

When determining the function of pressure change on the interchamber jumpers, the Reynolds equation [15, 16] was used, which was written in a dimensionless form

$$\frac{\partial}{\partial \varphi} \left(\frac{\overline{h}_i^3}{k_{zi}} \cdot \frac{\partial \overline{P}}{\partial \varphi} \right) + \frac{\partial}{\partial Z} \left(\frac{\overline{h}_i^3}{k_{zi}} \cdot \frac{\partial \overline{P}}{\partial Z} \right) = \Omega \frac{\partial (\overline{U} \cdot \overline{h}_i)}{\partial \varphi}, \quad (2)$$

where φ, Z – circular and axial coordinates in the bearing; \overline{h}_i – current values of clearances in the bearing; \overline{P} – current value of pressure on the interchamber jumpers; k_{zi}, k_{zi} – coefficients of turbulence of the lubricant flow; \overline{U} – circular speed of the rotating working surface.

The Reynolds equation (2) was solved numerically using approximate numerical methods, namely the finite differ-

ence method in combination with the longitudinal-transverse sweep method. The boundary conditions when solving the Reynolds equation were pressures in the chambers, which were determined from equation (1), and pressures at the ends of the bearing (that is, at the outlet of the working fluid).

To write equation (2) in the form of finite differences, the surfaces between the chambers were covered with a regular grid and the individual derivatives were recorded using a five-point template. The iterative process of determining the pressures on the interchamber bridges continued until the required accuracy was achieved, which was specified in advance.

Knowing pressure in the chambers and on the interchamber bridges, the load-bearing capacity of the bearing was determined by integrating the network function of the pressure distribution. The Simpson's method was used for integration.

Based on the known values of pressures in the chambers, the losses of the working fluid through the bearing were determined using the following equation

$$Q_{\Sigma} = \psi_{in} \cdot \pi \cdot r_k^2 \cdot \sqrt{\frac{2 \cdot P_1}{\rho}} \cdot \sum_{i=1}^k \sqrt{1 - \overline{P}_{k,i}}, \quad (3)$$

where ψ_{in} is the inlet coefficient;

r_k is the nozzle radius;

ρ is the working fluid density;

k is the number of chambers;

P_1 is the pressure at the inlet to the bearing from the pump.

The friction power losses were determined by double integration of the tangential stress function along the plane of the working friction surface.

The power losses for pumping the working fluid through the slotted path were determined from the following expression

$$N_{prok} = P_1 \cdot Q_{\Sigma}. \quad (4)$$

The mathematical model above has made it possible to determine values for the design and operational parameters of the hydrostatic bearing, which ensure its required load-bearing capacity.

5. Results of investigating the basic characteristics of a hydrostatic bearing of the satellite in an aircraft engine gearbox

5.1. Results of determining the basic characteristics of hydrostatic-dynamic bearings taking into account hydrodynamic and hydrostatic effects

The study of the bearing capacity, working fluid consumption, and power losses due to friction and pumping of the working fluid was carried out on the basis of the joint solution to the Reynolds equations and the balance of working fluid consumption. The pressure in the chambers was determined from the equation of equality of the working fluid consumption through the inlet pressure compensator and along the contour of the *i*-th chamber.

The turbulence of the lubricant flow was taken into account using the imperial formulae proposed by Konstantinescu.

On the interchamber bridges, the pressure in the lubricant layer was determined from the numerical solution to the Reynolds equation. The pressure in the chambers and on the

interchamber bridges was determined by an iterative method until the required accuracy was achieved.

The load-bearing capacity of the hydrostatic bearing was determined by integrating the mesh function of the pressure distribution over the bearing surface. The working fluid flow rate through the bearing was calculated based on the known pressure in the chambers. Friction power losses were determined by double integration of the tangential stresses in the lubricant layer over the surface of the hydrostatic bearing.

In a hydrostatic bearing, in addition to friction losses, there are losses for pumping the working fluid through the bearing path. They were determined by multiplying the working fluid pressure from the pump by the total working fluid flow rate through the bearing.

Calculations of the basic characteristics of the bearing were performed at the following values for design and operational parameters:

1. Working fluid pressure at the inlet to the bearing chambers $P_1 = (2...8)$ MPa.
2. Bearing diameter $d = 75$ mm.
3. Bearing length $L = 70$ mm.
4. Chamber length $l_k = 20$ mm.
5. Chamber width $b_k = 10$ mm.
6. Interchamber jumper width $L_{mk} = 48.9$ mm.
7. Nozzle diameter $d_k = 2.5$ mm.
8. Bearing clearance $\delta = 0.1$ mm.
9. Number of satellites – 4.
10. Number of chambers in one row $k = 4$ (there are 8 chambers in the bearing).
11. Satellite rotation frequency relative to the carrier $\omega = 1713.168 \text{ s}^{-1}$.
12. Shaft eccentricity in the bearing $x = 0.7$ (dimensionless).
13. Engine power $N = 1876$ kW.
14. Gear oil pump.
15. Working medium – oil mk – 8 at temperature $t = 75^\circ\text{C}$.
– dynamic viscosity of oil $\mu = 0.003458 \text{ N}\cdot\text{s}/\text{m}^2$;
– oil density $\rho = 869.6 \text{ kg}/\text{m}^3$.
16. Required bearing load capacity $W = 5438$ N.

The results of calculating the bearing load capacity depending on the pressure at the inlet to the bearing are shown in Fig. 2.

All the results and plots were constructed according to a single mathematical model. This model was based on the pressure distribution function over the working surface of the bearing. Given the initial data, the pressures in the chambers were calculated using formula (1). The pressures on the interchamber bridges were determined from the numerical solution to the Reynolds equation (2). On the end bridges, a linear law of pressure change was adopted. The bearing load capacity was determined as the sum of the load capacities of the chambers, interchamber, and end bridges, and was recorded in projections onto the vertical y axis (I) and the horizontal x axis (J) (5). Taking into account the fact that the working surface of the bearing had two rows of chambers, the total load capacity was multiplied by two

$$I = (W_{y_{kam}} + W_{y_m} + W_{y_t} + W_{y_p}) \cdot 2,$$

$$J = (W_{x_{kam}} + W_{x_m} + W_{x_t} + W_{x_p}) \cdot 2, \tag{5}$$

where $W_{y_{kam}}$ and $W_{x_{kam}}$ are the load-bearing capacities of the chambers in the projections onto the y and x axes;

W_{y_m}, W_{x_m} are the load-bearing capacities of the interchamber jumpers in the projections on the y and x axes;

W_{y_p}, W_{x_p} are the load-bearing capacities of the end interchamber jumpers in the projections onto the y and x axes.

The power losses due to friction were determined by double integration of the tangential stress distribution function (6)

$$N_p = \omega \cdot R \cdot \iint \tau dS, \tag{6}$$

where τ is the tangential stress distribution function in the working fluid layer;

S is the friction surface area;

ω is the angular velocity of rotation of the moving surface;

R is the radius of the friction surface.

The tangential stress distribution function τ according to Newton's law takes the following form (7)

$$\tau = \frac{\mu \cdot U}{h} + \frac{h}{2} \frac{dP}{dX}, \tag{7}$$

where $U = \omega R$ – circumferential speed;

μ – dynamic viscosity of the working fluid;

h – current clearance in the bearing;

$\frac{dP}{dX}$ – pressure gradient of the working fluid in the circumferential direction.

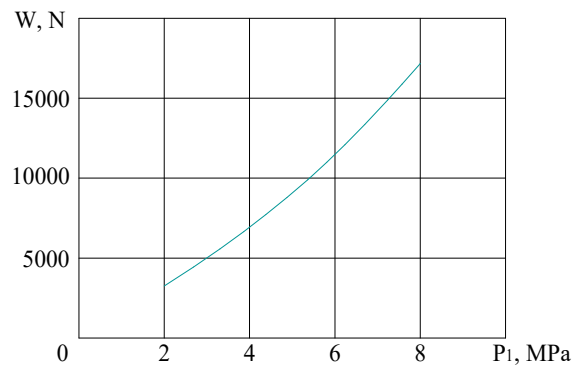


Fig. 2. Dependence of bearing load capacity on the pressure at the inlet to a hydrostatic bearing

Numerically, the power losses due to friction were determined using the trapezoidal formula.

The dependence of working fluid consumption and power losses due to friction and pumping on the pressure at the inlet to a hydrostatic bearing is shown in Fig. 3, 4.

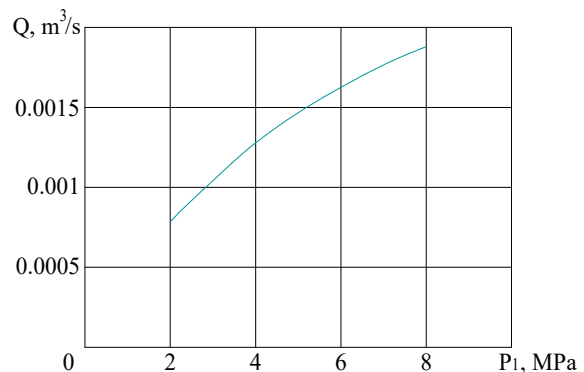


Fig. 3. Dependence of working fluid flow rate on the pressure at the inlet to the hydrostatic bearing

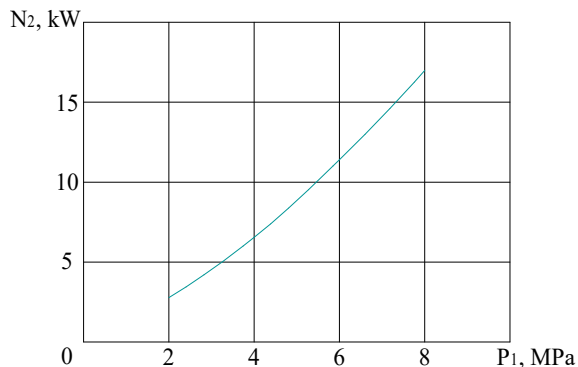


Fig. 4. Dependence of power losses due to friction and pumping on the pressure at the inlet to the hydrostatic bearing

5. 2. Results of investigating the influence of nozzle diameter on the basic characteristics of a hydrostatic bearing in the gearbox satellite

The values of nozzle diameters in the bearings were determined based on the accumulated experience of theoretical and experimental research into hydrostatic bearings. The results from calculating the bearing load capacity, working fluid consumption, and power losses due to friction and pumping are shown in Fig. 5–7.

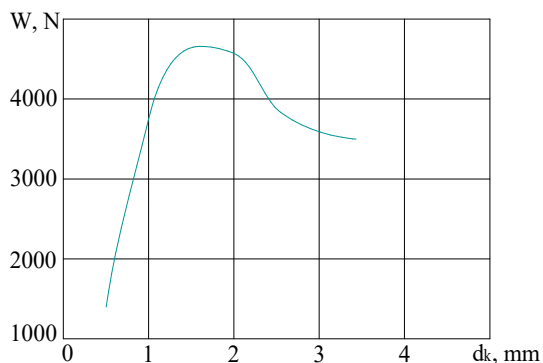


Fig. 5. Dependence of bearing load capacity on the diameter of the nozzle installed at the inlet to the bearing chambers

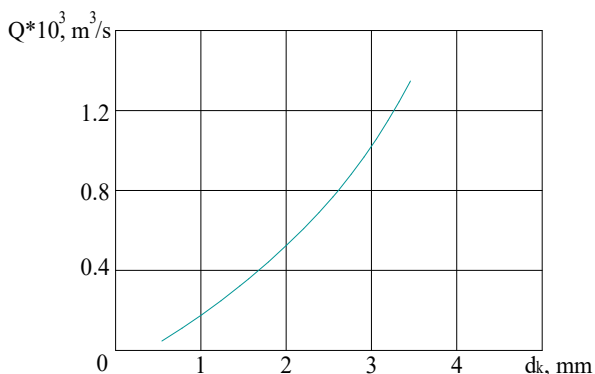


Fig. 6. Dependence of working fluid flow rate on the nozzle diameter in a hydrostatic bearing

Fig. 5 demonstrates that for a given clearance, there is an optimal value of the nozzle diameter, which provided the maximum value of the bearing load capacity. The optimal value of the nozzle diameter depends on many parameters and must be determined for each bearing design separately.

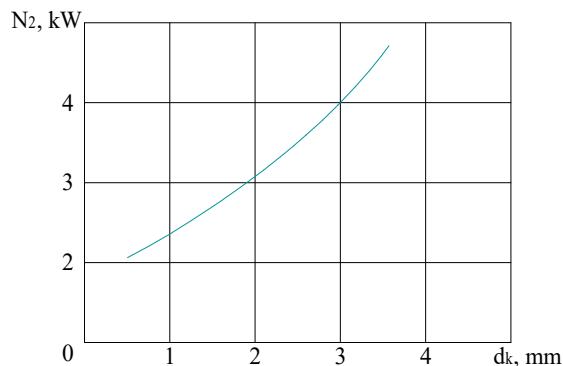


Fig. 7. Dependence of power losses due to friction and pumping on the nozzle diameter in a hydrostatic bearing

6. Discussion of results based on investigating the characteristics of a hydrostatic bearing in the satellites of an aviation gearbox

In contrast to [15, 16], in which single-row hydrostatic bearings that operate on fuel are considered, this paper considers a double-row hydrostatic bearing that operates on the oil system of the engine. This result makes it possible to obtain a high load capacity of the support of the satellite, which perceives very large loads. The oil system of the engine makes it possible to ensure the operation of the bearing with a working fluid.

A feature of the proposed calculation procedure is the assessment of the possibility of using hydrostatic bearings in the supports of satellites in aviation gearboxes. The structure of the support of satellites has been designed and the algorithm for calculating the main parameters of the hydrostatic bearing of the satellites was developed for different pressure values of the working fluid and the diameters of the jets at the inlet to the bearing chambers. The above analysis of the influence of the structural and operational parameters of the hydrostatic bearing on its characteristics in relation to the supports of aircraft engine satellites was not considered in [1–14]. The results of the calculations showed that the hydrostatic bearing can be used in the supports of satellites in aviation gearboxes.

The results from calculating the bearing capacity, working fluid consumption, and power losses due to friction and pumping of the hydrostatic bearing are shown in Fig. 2–7. Fig. 2 demonstrates that with an increase in the pressure at the inlet to the bearing chambers, its load-bearing capacity increases. The required load-bearing capacity of the bearing is provided at a pressure at the inlet to the bearing chambers of approximately 3 MPa. Fig. 3, 4 show that with an increase in the pressure at the inlet to the hydrostatic bearing from 2 MPa to 8 MPa, the working fluid consumption increases by 2.5 times, and the power losses due to friction and pumping increase by 6.8 times.

However, the total power losses due to friction and pumping for 4 satellites are 1.066% of the total engine power.

Fig. 5 demonstrates that when studying the influence of the nozzle diameter on the bearing capacity of the bearing, its optimal value was found. In this case, it is desirable to set the nozzle diameter from 1.5 mm to 2 mm. Fig. 5 also shows that the nozzle diameter can significantly affect the load-bearing capacity of the hydrostatic bearing, especially to the left of the optimal nozzle diameter value.

Fig. 6 demonstrates that the nozzle diameter significantly affects the flow rate of the working fluid through the bearing. When the nozzle diameter increases from 0.5 mm to 3.5 mm, the flow rate of the working fluid increases by 22.8 times. Fig. 7 shows that in the studied range of nozzle diameters, the power losses due to friction and pumping increased by 2.1 times, with an increase in the nozzle diameter.

The flow of lubricant in a hydrostatic-dynamic bearing is determined by two factors: the relative movement of the shaft and the working surface of the bearing, as well as pressure drops acting in the circumferential and axial directions. The simultaneous existence of these flows affects the characteristics of the lubricating film. Unlike hydrodynamic bearings, in which the velocities of pressure flows are small, in hydrostatic-dynamic bearings, regardless of their speed, the average flow rates of pressure and shear flows are not directly related to each other. The above-mentioned difference in the behavior of pressure and shear flows requires a differentiated approach to determining the characteristics of flows caused by the manifestation of both factors.

In hydrostatic-dynamic bearings, the working fluid is supplied under high pressure. As the supply pressure of the working fluid increases, the viscosity of the working fluid increases. The viscosity of the working fluid increases the more the greater the pressure under which the working fluid is supplied to the bearing. The basis for determining the characteristics of a hydrostatic-dynamic bearing is the function of the pressure distribution in the lubricant layer. As the viscosity of the working fluid increases, the pressure in the lubricant layer increases and the bearing capacity increases. In the mathematical model of a hydrostatic-dynamic bearing, the fluid flow rate along the contour of the i -th chamber is recorded taking into account the transfer and gradient flow, as well as the viscosity of the working fluid. Therefore, with increasing pressure, the bearing capacity of the bearing (Fig. 2) increases. The same effect is given by changing the nozzle diameter. When the nozzle diameter changes, the pressure in the bearing chambers of the hydrostatic-dynamic bearing changes.

The absence of an experimental part is explained by the need to solve very complex issues and significantly improve the experimental bench. It is necessary to manufacture a new bearing structure, design a new system for supplying and removing the working fluid, and improve the system for measuring the bearing parameters. However, the extensive experience of conducting experimental studies involving other structures of hydrostatic dynamic bearings, the results of which were confirmed by theoretical research, allows me to consider current theoretical study reliable.

The results showed that the hydrostatic bearing can be used in the supports of satellites in aviation gearboxes.

The advantage of this study is a comprehensive approach, which is associated with the determination of the engagement forces and external load on the hydrostatic bearing. A complex hydromechanical problem has been solved.

A limitation of this work is the need for thorough cleaning of the working fluid and the likelihood of clogging of the nozzle. For bearings with other design parameters, the

results and conclusions will not change qualitatively. The difference can only be in quantitative indicators.

The disadvantage of this study is the failure to take into account the centrifugal force in the engagement when determining the external load on the bearing.

Future studies might take into account the dynamic phenomena that arise during the operation of an aircraft gearbox.

7. Conclusions

1. It has been established that with an increase in the pressure at the inlet to the bearing, its load-bearing capacity increases, and the required bearing capacity of the bearing is provided at a pressure at the inlet to the bearing chambers of approximately 3 MPa. With an increase in pressure from 2 MPa to 8 MPa, the working fluid consumption increases by 2.5 times, and the power losses due to friction and pumping increase by 6.8 times. The total power losses due to friction and pumping are 1.066% of the total engine power.

2. The optimal value of the nozzle diameter has been established, which provides the maximum value of the bearing capacity of the bearing. In this case, the nozzle diameter is preferably set in the range from 1.5 mm to 2 mm. When the nozzle diameter increases from 0.5 mm to 3.5 mm, the working fluid consumption increases by 22.8 times, and the power losses due to friction and pumping increase by 2.1 times.

Conflicts of interest

The author declares that he has no conflicts of interest in relation to the current study, including financial, personal, authorship, or any other, that could affect the study and the results reported in this paper.

Funding

The study was conducted without financial support.

Data availability

All data are available in the main text of the manuscript.

Use of artificial intelligence

The author confirms that he did not use artificial intelligence technologies when creating the current work.

Author's contribution

Vladimir Nazin: Conceptualization, Methodology, Software, Formal analysis.

References

- Gong, J., Liu, K., Meng, F., Wang, H., Xu, H. (2024). Effect of meshing-induced deformation on lubrication for journal planet gear bearings. *International Journal of Mechanical Sciences*, 284, 109747. <https://doi.org/10.1016/j.ijmecsci.2024.109747>

2. Liu, J., Ding, S., Wang, L., Li, H., Xu, J. (2019). Effect of the bearing clearance on vibrations of a double-row planetary gear system. *Proceedings of the Institution of Mechanical Engineers, Part K: Journal of Multi-Body Dynamics*, 234 (2), 347–357. <https://doi.org/10.1177/1464419319893488>
3. Li, X., Liu, J., Xu, J., Chen, Y., Hu, Z., Pan, G. (2023). A vibration model of a planetary bearing system considering the time-varying wear. *Nonlinear Dynamics*, 111 (21), 19817–19840. <https://doi.org/10.1007/s11071-023-08845-5>
4. Liu, J., Xu, Y., Shao, Y., Xiao, H., Li, H. (2018). The effect of a localized fault in the planet bearing on vibrations of a planetary gear set. *The Journal of Strain Analysis for Engineering Design*, 53 (5), 313–323. <https://doi.org/10.1177/0309324718769491>
5. Li, H., Tan, J., Fei, W., Zhu, C., Sun, Y., Sun, Z. (2025). Collaborative optimization of meshing and lubrication for planetary gear-journal bearing integrated structure in high power density wind turbine drivetrains. *Renewable Energy*, 255, 123763. <https://doi.org/10.1016/j.renene.2025.123763>
6. Chen, Q., Zhang, K., Zhang, Y., Ding, Q., Zhu, Y., Feng, K. (2024). Full-Size Experimental Investigations on Planetary Gear Journal Bearings in High-Power Wind Turbines. *Journal of Tribology*, 147 (3). <https://doi.org/10.1115/1.4066648>
7. Zhou, C., Wang, R., Fu, D., Zhao, N., Ma, X. (2025). Joint Modeling of Planetary Gear Train and Bearings of Wind Turbines for Vibration Analysis of Planetary Bearing Outer Ring Looseness Fault. *Energies*, 18 (22), 5938. <https://doi.org/10.3390/en18225938>
8. Tchufistov, E. A., Tchufistov, O. E. (2020). Simulation of satellite bearings loading in planetary cycloid gear. *IOP Conference Series: Materials Science and Engineering*, 971 (4), 42048. <https://doi.org/10.1088/1757-899x/971/4/042048>
9. Ding, H., Mermertas, Ü., Hagemann, T., Schwarze, H. (2024). Calculation and Validation of Planet Gear Sliding Bearings for a Three-Stage Wind Turbine Gearbox. *Lubricants*, 12 (3), 95. <https://doi.org/10.3390/lubricants12030095>
10. Suzuki, A., Aoyama, T., Sugiura, N., Inagaki, M., Shimizu, T. (2011). Influence of Bearing Clearance on Load Sharing in Planetary Gears. Volume 8: 11th International Power Transmission and Gearing Conference; 13th International Conference on Advanced Vehicle and Tire Technologies, 259–265. <https://doi.org/10.1115/detc2011-47622>
11. Fingerle, A., Hochrein, J., Otto, M., Stahl, K. (2019). Theoretical Study on the Influence of Planet Gear Rim Thickness and Bearing Clearance on Calculated Bearing Life. *Journal of Mechanical Design*, 142 (3). <https://doi.org/10.1115/1.4045244>
12. Keller, J., Guo, Y., Zhang, Z., Lucas, D. (2018). Comparison of planetary bearing load-sharing characteristics in wind turbine gearboxes. *Wind Energy Science*, 3 (2), 947–960. <https://doi.org/10.5194/wes-3-947-2018>
13. Jang, J. Y., Khonsari, M. M. (2020). On the wear of dynamically-loaded engine bearings with provision for misalignment and surface roughness. *Tribology International*, 141, 105919. <https://doi.org/10.1016/j.triboint.2019.105919>
14. Dong, P., Lai, J., Guo, W., Tenberge, P., Xu, X., Liu, Y., Wang, S. (2023). An analytical approach for calculating thin-walled planet bearing load distribution. *International Journal of Mechanical Sciences*, 242, 108019. <https://doi.org/10.1016/j.ijmecsci.2022.108019>
15. Nazin, V. (2024). Identifying the influence of design parameters of single-chamber hydrostatic bearing of fuel pump on its main characteristics. *Eastern-European Journal of Enterprise Technologies*, 1 (7 (127)), 30–36. <https://doi.org/10.15587/1729-4061.2024.298646>
16. Nazin, V. (2023). Revealing the influence of structural and operational parameters of a hydrostatic bearing in a gear-type fuel pump on its main characteristics. *Eastern-European Journal of Enterprise Technologies*, 2 (1 (122)), 92–98. <https://doi.org/10.15587/1729-4061.2023.277755>